

# Solubility and Diffusivity of Difluoromethane in Room-Temperature Ionic Liquids

Mark B. Shiflett,<sup>\*,†</sup> Mark A. Harmer,<sup>†</sup> Christopher P. Junk,<sup>†</sup> and A. Yokozeki<sup>‡</sup>

DuPont Central Research and Development, Experimental Station, Wilmington, Delaware 19880, and DuPont Fluoroproducts Laboratory, Chestnut Run Plaza 711, Wilmington, Delaware 19880

New experimental results are presented for the solubility and diffusivity of difluoromethane in 19 room-temperature ionic liquids (RTILs). In the series of RTILs presented here, eight RTILs with five new fluorocarbon sulfonate anions have been prepared for the first time. The measurements were performed using a gravimetric microbalance at temperatures between (283.15 and 348.15) K and at pressures from (0.01 to 1.0) MPa. Experimental gas solubility data were successfully correlated with the nonrandom two-liquid (NRTL) solution model. The solubility of difluoromethane in RTILs is affected by the choice of both the cation and anion. Diffusivities obtained from the time-dependent absorption data were well analyzed using a model based on a modified Stokes–Einstein equation. The calculated molecular size for difluoromethane is 2 to 3 times larger than the known size.

## Introduction

Gas solubility and diffusivity data with various RTILs are critically important and needed to develop new applications.<sup>1–11</sup> In our previous work,<sup>12</sup> we showed for the first time that large differences in gas solubility exist for hydrofluorocarbons (HFCs) in two common RTILs, 1-butyl-3-methylimidazolium hexafluorophosphate [bmim][PF<sub>6</sub>] and 1-butyl-3-methylimidazolium tetrafluoroborate [bmim][BF<sub>4</sub>]. Among the HFCs studied, which included trifluoromethane (R-23), difluoromethane (R-32), pentafluoroethane (R-125), 1,1,1,2-tetrafluoroethane (R-134a), 1,1,1-trifluoroethane (R-143a), and 1,1-difluoroethane (R-152a), R-32 had the highest gas solubility (R-32 > R-152a > R-23 > R-134a > R-125 > R-143a). The trend in solubility did not correlate with the HFCs dipole moment as expected; however, the unique H-bonding capability (H–F–H) of HFCs is believed to be involved. In this paper, we continue to investigate the solubility and diffusivity of R-32 in 19 RTILs in order to gain further insight into these molecular interactions. Eleven commercially available RTILs ([bmim][PF<sub>6</sub>], [bmim][BF<sub>4</sub>], 1,2-dimethyl-3-propylimidazolium tris(trifluoromethylsulfonyl)methide [dmpim][TMeM] or [dmpim][Tf<sub>3</sub>C], 1-ethyl-3-methylimidazolium bis(pentafluoroethylsulfonyl)imide [emim][BEI], 1,2-dimethyl-3-propylimidazolium bis(trifluoromethylsulfonyl)imide [dmpim][BMeI] or [dmpim][Tf<sub>2</sub>N], 1-ethyl-3-methylimidazolium bis(trifluoromethylsulfonyl)imide [emim][BMeI] or [emim][Tf<sub>2</sub>N], 3-methyl-1-propylpyridinium bis(trifluoromethylsulfonyl)imide [pmpy][BMeI] or [pmpy][Tf<sub>2</sub>N], 1-butyl-3-methylpyridinium bis(trifluoromethylsulfonyl)imide, [bmpy][BMeI] or [bmpy][Tf<sub>2</sub>N], 1-butyl-3-methylimidazolium acetate [bmim][Ac], 1-butyl-3-methylimidazolium thiocyanate [bmim][SCN], and 1-butyl-3-methylimidazolium methyl sulfate [bmim][MeSO<sub>4</sub>]) were included in this study. In addition, eight new RTILs (1-ethyl-3-methylimidazolium 1,1,2,2-tetrafluoroethanesulfonate [emim][TFES], 1-butyl-3-methylimidazolium 1,1,2,2-tetrafluoroethanesulfonate [bmim][TFES], 1-heptyl-3-methylimidazolium 1,1,2,2-tetrafluoroethanesulfonate [hmim][TFES], 1-dodecyl-3-methylimidazolium 1,1,2,2-tetrafluoroethanesulfonate

[dmim][TFES], 1-butyl-3-methylimidazolium 1,1,2,3,3,3-hexafluoropropanesulfonate [bmim][HFPS], 1-butyl-3-methylimidazolium 2-(1,2,2,2-tetrafluoroethoxy)-1,1,2,2-tetrafluoroethanesulfonate [bmim][FS], 1-butyl-3-methylimidazolium 1,1,2-trifluoro-2-(perfluoroethoxy)ethanesulfonate [bmim][TPES], 1-butyl-3-methylimidazolium 1,1,2-trifluoro-2-(trifluoromethoxy)ethanesulfonate [bmim][TTES]) were synthesized to evaluate the (H–F–H) interaction between the fluorinated anions and difluoromethane. Table 1 provides the chemical name, CAS Registry Number (CASRN), source, abbreviation, structure, and molecular weight of the 19 ionic liquids that were studied.

In addition to our own work, only two literature references are known regarding the interaction (electrical conductivity) of R-32 in a RTIL.<sup>13,14</sup> The present study is the first systematic investigation of the solubility and diffusivity of R-32, in a variety of RTILs with both fluorinated and nonfluorinated anions. Similar to our previous work,<sup>12</sup> we analyze the observed solubility data with the conventional NRTL solution (activity coefficient) model and successfully analyze the observed diffusivity behavior with a simple semi-theoretical model.

## Experimental Procedures

**Apparatus and Measuring Technique.** A detailed description of the experimental equipment and procedure is available in our previous paper.<sup>15</sup> Therefore, only the basic experimental technique and experimental uncertainties are given here.

The gas solubility and diffusivity measurements were made using a gravimetric microbalance (Hiden Isochema Ltd, IGA 003).<sup>16</sup> Initially, (60 to 80) mg of ionic liquid was loaded into the sample container and heated to 348.15 K under a vacuum of about 10<sup>−9</sup> MPa for 10 h to remove any trace amounts of water or other impurities. For example, [bmim][TFES] with an initial mass of 68.4661 mg was dried with a final dry mass of 66.7138 mg resulting in a mass fraction loss of 0.025. The initial as-received mass fraction of water measured by Karl Fischer titration (Aqua-Star C3000, solutions Aqua-Star Coulomat C and A) was 0.019; therefore the majority of the measured mass loss is due to the removal of water. The as-received mass fraction of water for all samples ranged from (0.001 to 0.02); therefore, the samples were carefully dried according to the

\* Corresponding author. E-mail: mark.b.shiflett@usa.dupont.com.

<sup>†</sup> DuPont Central Research and Development.

<sup>‡</sup> DuPont Fluoroproducts Laboratory.

Table 1. Nineteen Ionic Liquids Studied

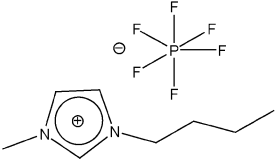
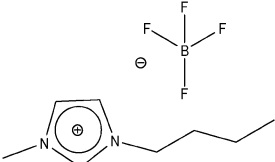
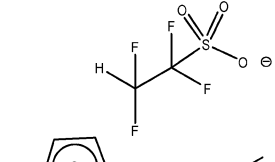
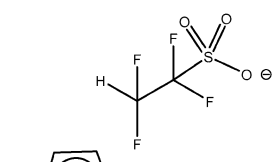
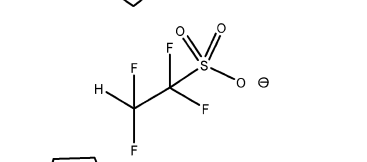
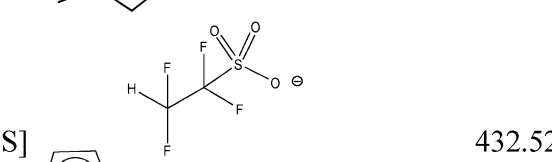
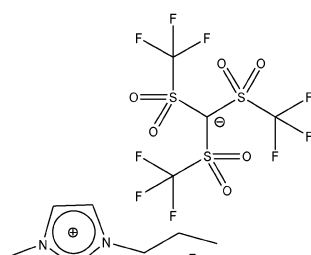
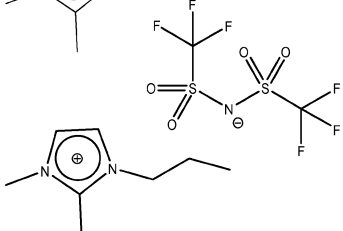
Chemical Name	Abbreviation	Structure	MW
1-butyl-3-methylimidazolium hexafluorophosphate <sup>a)</sup> CAS# 174501-64-5	[bmim][PF <sub>6</sub> ]		284.18
1-butyl-3-methylimidazolium tetrafluoroborate <sup>a)</sup> CAS# 174501-65-6	[bmim][BF <sub>4</sub> ]		226.03
1-butyl-3-methylimidazolium 1,1,2,2-tetrafluoroethanesulfonate <sup>b)</sup>	[bmim][TFES]		320.30
1-ethyl-3-methylimidazolium 1,1,2,2-tetrafluoroethanesulfonate <sup>b)</sup>	[emim][TFES]		292.25
1-heptyl-3-methylimidazolium 1,1,2,2-tetrafluoroethanesulfonate <sup>b)</sup>	[hmim][TFES]		362.38
1-dodecyl-3-methylimidazolium 1,1,2,2-tetrafluoroethanesulfonate <sup>b)</sup>	[dmim][TFES]		432.52
1,2-dimethyl-3-propylimidazolium tris(trifluoromethylsulfonyl)methide <sup>a)</sup> CAS# 169051-77-8	[dmpim][TMeM]		551.45
1,2-dimethyl-3-propylimidazolium bis(trifluoromethylsulfonyl)imide <sup>a)</sup> CAS# 169051-76-7	[dmpim][BMeI]		419.36

Table 1. (Continued)

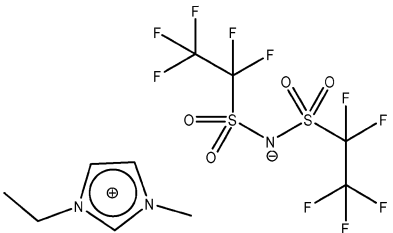
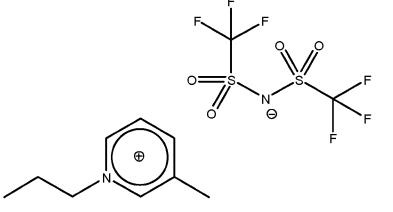
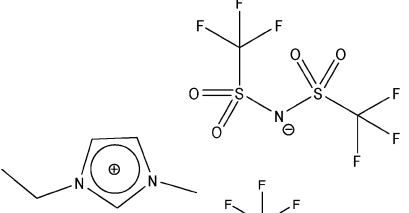
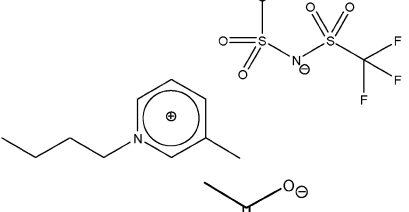
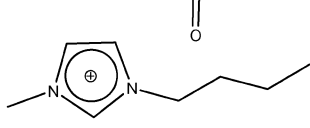
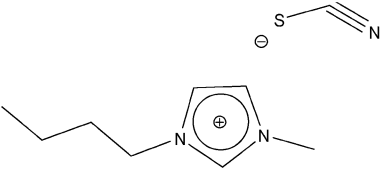
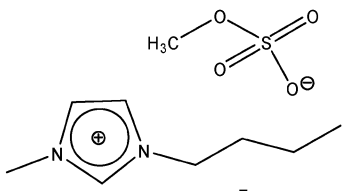
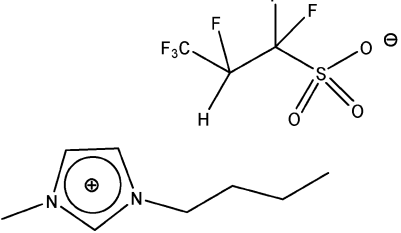
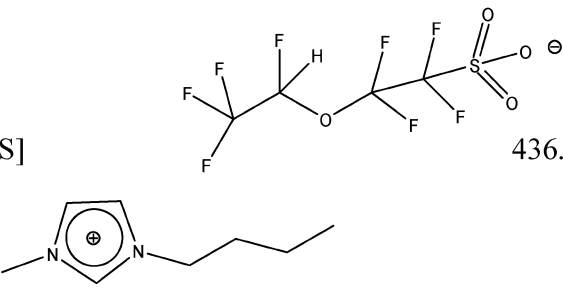
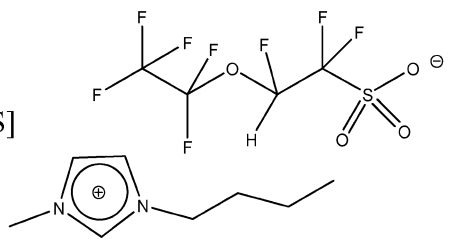
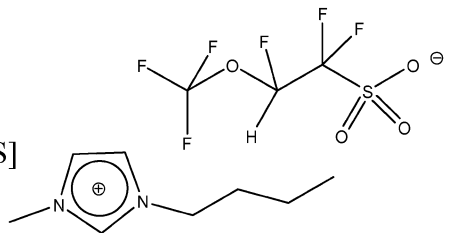
Chemical Name	Abbreviation	Structure	MW
1-ethyl-3-methylimidazolium bis(pentafluoroethylsulfonyl)imide <sup>a)</sup>	[emim][BEI]		491.33
CAS# 216299-76-2			
3-methyl-1-propylpyridinium bis(trifluoromethylsulfonyl)imide <sup>a)</sup>	[pmpy][BMeI]		416.40
CAS# 817575-06-7			
1-ethyl-3-methylimidazolium bis(trifluoromethylsulfonyl)imide <sup>a)</sup>	[emim][BMeI]		391.31
CAS# 174899-82-2			
1-butyl-3-methylpyridinium bis(trifluoromethylsulfonyl)imide <sup>a)</sup>	[bmpy][BMeI]		430.39
CAS# 344790-86-9			
1-butyl-3-methylimidazolium acetate <sup>a)</sup>	[bmim][Ac]		198.26
CAS# 284049-75-8			
1-butyl-3-methylimidazolium thiocyanate <sup>a)</sup>	[bmim][SCN]		197.30
CAS# 344790-87-0			
1-butyl-3-methylimidazolium methyl sulfate <sup>a)</sup>	[bmim][MeSO <sub>4</sub> ]		250.32
CAS# 401788-98-5			
1-butyl-3-methylimidazolium 1,1,2,3,3,3-hexafluoropropanesulfonate <sup>b)</sup>	[bmim][HFPS]		370.31

Table 1. (Continued)

Chemical Name	Abbreviation	Structure	MW
1-butyl-3-methylimidazolium 2-(1,2,2,2-tetrafluoroethoxy)-1,1,2,2-tetrafluoroethanesulfonate <sup>b)</sup>	[bmim][FS]		436.32
1-butyl-3-methylimidazolium 1,1,2-trifluoro-2-(perfluoroethoxy)ethanesulfonate <sup>b)</sup>	[bmim][TPES]		436.32
1-butyl-3-methylimidazolium 1,1,2-trifluoro-2-(trifluoromethoxy)ethanesulfonate <sup>b)</sup>	[bmim][TTES]		386.31

<sup>a</sup> Fluka Chemika. <sup>b</sup> DuPont.

stated experimental procedure prior to measuring the isotherms. An isotherm was measured at 298.15 K over a pressure range from about (0.01 to 1.0) MPa. Three additional isotherms were measured at (283.15, 323.15, and 348.15) K over the same pressure range for ionic liquids with high R-32 gas solubility at 298.15 K. The upper pressure limit for R-32 was dependent on the saturation pressure in the sample container at ambient temperature (1.5 MPa at 294.3 K). To ensure sufficient time for gas–liquid equilibrium, the ionic liquid samples were maintained at each pressure set-point for a minimum of 3 h and a maximum of 10 h.

The instrumental uncertainties in  $T$  and  $P$  are within 0.1 K and 0.8 kPa, respectively. These uncertainties do not cause any significant changes in the gas solubility measurement. One of the largest sources of uncertainty in the present experiment is reproducibility. We have examined the reproducibility by repeating the [dmpim][TMeM] isotherm in different times (for example, several months apart for the same binary system). Our best estimate for the present experimental reproducibility, including the sample (ionic liquid) purity effect, has been less than 0.006 mole fraction. The next largest systematic uncertainty is due to the buoyancy correction in the data analysis. A detailed description of the buoyancy correction is provided in our previous reports,<sup>12,15</sup> and total uncertainties in the solubility data due to both random and systematic errors have been estimated to be less than 0.006 mole fraction at given  $T$  and  $P$ .

Concerning uncertainties in the diffusivity data, the largest uncertainty source comes from experimental reproducibility (random) errors. These were estimated to be roughly within a factor of 2 in the determined diffusivity, based on the scatters of various analyzed diffusivity data. These erratic time-

dependent data were not included in the analysis. The second largest uncertainty source in the diffusivity data is due to the liquid-depth parameter,  $L$  in the analysis, which was assumed to be constant. However,  $L$  varies with the amount of gas absorption, due to the liquid expansion by the gas absorption. Uncertainties by this variable  $L$  in the analysis showed less than about 60 % effect in the final diffusivity data. Thus, the overall uncertainty limit in the diffusivity of a factor of 2, cited above, will cover this systematic error as well.

Analysis of the buoyancy effects requires an accurate measurement of the RTIL density. Densities of RTILs were measured at four temperatures (283.15, 298.15, 323.15, and 348.15) K using an oscillating u-tube density meter (Microdensity meter, model 102B) and also verified at 298.15 K using a helium pycnometer (Micromeritics AccuPyc 1330 with a 1 cm<sup>3</sup> measuring cup). The sample densities and linear correlations for the multi-temperature density measurements are provided in Table 2. Additional, single-temperature density measurements at about (298.15 to 301.45) K are provided in Table 3. The uncertainties in both density methods are  $\pm 0.001$  g·cm<sup>-3</sup>.

To correlate our diffusivity measurements, absolute viscosity data for RTILs are required. In our previous work,<sup>15</sup> we measured the viscosity for [bmim][PF<sub>6</sub>] and [bmim][BF<sub>4</sub>] using a falling needle viscometer (Stony Brook Scientific, DV-100) over a temperature range from (283.15 to 348.15) K. In this work, we measure the viscosity for [bmim][PF<sub>6</sub>], [bmim][BF<sub>4</sub>], [dmpim][TMeM], [emim][BEI], [emim][BMeI], and [pmpy]-[BMeI] using a capillary viscometer (Cannon-Manning semi-micro viscometer) over a temperature range from (283.15 to 373.15) K.<sup>17</sup> The uncertainty in the viscosity measurement was  $\pm 5$  % over the entire temperature range measured. We found

**Table 2. Multi-Temperature Density Measurements**

abbreviation	<i>T</i> /K	$\rho/\text{g}\cdot\text{cm}^{-3}$ <sup>a</sup>	
[bmim][HFPS]	283.15	1.422	$\rho/\text{g}\cdot\text{cm}^{-3} = 1.678 - 9.057 \times 10^{-4} (T/K)^b$
	298.15	1.409	
	323.15	1.385	
	348.15	1.364	
[bmim][FS]	283.15	1.464	$\rho/\text{g}\cdot\text{cm}^{-3} = 1.738 - 9.675 \times 10^{-4} (T/K)^b$
	298.15	1.449	
	323.15	1.425	
	348.15	1.401	
[bmim][TPES]	283.15	1.439	$\rho/\text{g}\cdot\text{cm}^{-3} = 1.727 - 1.021 \times 10^{-3} (T/K)^b$
	298.15	1.423	
	323.15	1.397	
	348.15	1.372	
[bmim][TTES]	283.15	1.409	$\rho/\text{g}\cdot\text{cm}^{-3} = 1.685 - 9.764 \times 10^{-4} (T/K)^b$
	298.15	1.393	
	323.15	1.369	
	348.15	1.345	
[dmpim][TMeM]	283.15	1.612	$\rho/\text{g}\cdot\text{cm}^{-3} = 1.803 - 6.804 \times 10^{-4} (T/K)^b$
	298.15	1.597	
	323.15	1.582	
	348.15	1.567	
[emim][BEI]	283.15	1.608	$\rho/\text{g}\cdot\text{cm}^{-3} = 1.926 - 1.125 \times 10^{-3} (T/K)^b$
	298.15	1.590	
	323.15	1.562	
	348.15	1.534	
[pmpy][BMeI]	283.15	1.460	$\rho/\text{g}\cdot\text{cm}^{-3} = 1.730 - 9.560 \times 10^{-4} (T/K)^b$
	298.15	1.444	
	323.15	1.420	
	348.15	1.397	
[emim][BMeI]	283.15	1.534	$\rho/\text{g}\cdot\text{cm}^{-3} = 1.823 - 1.023 \times 10^{-3} (T/K)^b$
	298.15	1.517	
	323.15	1.492	
	348.15	1.467	
[bmpy][BMeI]	283.15	1.428	$\rho/\text{g}\cdot\text{cm}^{-3} = 1.689 - 9.253 \times 10^{-4} (T/K)^b$
	298.15	1.412	
	323.15	1.389	
	348.15	1.367	

<sup>a</sup> Microdensity meter (model 102). <sup>b</sup> Temperature range (283 < *T* < 348 K).

**Table 3. Single-Temperature Density Measurements**

abbreviation	<i>T</i> /K	$\rho/\text{g}\cdot\text{cm}^{-3}$ <sup>a</sup>
[bmim][TFES]	301.45	1.324
[emim][TFES]	301.45	1.502
[hmim][TFES]	301.15	1.274
[dmim][TFES]	301.35	1.136
[dmpim][BMeI]	299.15	1.481
[bmim][Ac]	298.15	1.053
[bmim][SCN]	298.65	1.067
[bmim][MeSO <sub>4</sub> ]	298.15	1.214

<sup>a</sup> Helium pycnometry (Micromeritics Accupyc 1330).

the capillary viscometer had two distinct advantages compared with the falling needle viscometer. First, the semi-micro viscometer requires only small amounts of ionic liquid (i.e., 0.5 mL to 1.0 mL) as compared with the falling needle viscometer (i.e., 5 mL to 10 mL). Second, the viscometer tubes could be sealed once the ionic liquid was loaded and dried to prevent exposure to air, which could reintroduce moisture back into the sample. The samples were carefully dried by connecting the viscometer u-tube to a turbo vacuum pump (Pfeiffer, model TSH 071). The viscometer tube was heated to 348.15 K under a vacuum of about 10<sup>-9</sup> MPa for 18 h to remove any trace amounts of water or other volatile impurities. Viscosity measurements are particularly sensitive to water contamination.<sup>18-20</sup> The initial viscosity measurements we reported for [bmim][PF<sub>6</sub>] and [bmim][BF<sub>4</sub>] in our previous publication<sup>12</sup> contained an unknown amount of water that reduced the viscosity as compared with our new measurements; therefore, the data reported in this work should be used in the future.

**Samples and Synthesis.** Difluoromethane was obtained from DuPont Fluoroproducts with a minimum purity of 0.999. A

molecular sieve trap was installed to remove any trace amounts of water from the gas. The RTILs obtained from Fluka Chemika have stated purities of > 0.97. Eight RTILs were prepared according to the following methods. The cation salts were obtained from Fluka Chemika and Acros Organics. The anion salts were synthesized by DuPont. The molecular structure was verified by nuclear magnetic resonance (NMR) and the stability by thermogravimetric analysis (TGA). <sup>19</sup>F NMR and <sup>1</sup>H NMR spectra were recorded on a Bruker model DRX-400 spectrometer at 376.8937 and 400.550 MHz, respectively using trichloromethane (CFCl<sub>3</sub>) as an internal standard and deuterated chloroform (CDCl<sub>3</sub>) as a lock solvent unless otherwise noted. A TA Instruments Q500 TGA was used to measure the change in mass of the ionic liquid as a function of temperature and atmosphere (air and nitrogen). Extractable chlorine content was measured by ion chromatography using a Dionex AS17 column.

**Preparation of 1-Butyl-3-methylimidazolium 1,1,2,2-Tetrafluoroethanesulfonate [bmim][TFES].** 1-Butyl-3-methylimidazolium chloride ([bmim][Cl]), 0.99 purity, Fluka, CASRN 79917-90-1, 60.0 g, 0.3435 mol) and high-purity dry acetone (> 0.995 purity, Aldrich, 300 mL) were combined in a 1 L flask and warmed to reflux with magnetic stirring until the solid all dissolved. At room temperature (293 K) in a separate 1 L flask, potassium 1,1,2,2-tetrafluoroethanesulfonate (TFES-K, 75.6 g, 0.344 mol) was dissolved in high-purity dry acetone (500 mL). These two solutions were combined at 293 K and allowed to stir magnetically for 2 h under positive nitrogen pressure. The stirring was stopped, and the KCl precipitate was allowed to settle and was then removed by suction filtration through a fritted glass funnel with a Celite pad. The acetone was removed in vacuo to give a yellow oil. The oil was further purified by diluting with high-purity acetone (100 mL) and stirring with decolorizing carbon (5 g). The mixture was again suction filtered, and the acetone was removed in vacuo to give a colorless oil. This was further dried at 4 Pa and 298.15 K for 6 h to provide 83.6 g of product.

<sup>19</sup>F NMR (DMSO-*d*<sub>6</sub>)  $\delta$  [ppm]: -124.7 (dt, *J* = 6 Hz, *J* = 8 Hz, 2F); -136.8 (dt, *J* = 53 Hz, 2F). <sup>1</sup>H NMR (DMSO-*d*<sub>6</sub>)  $\delta$  [ppm]: 0.9 (t, *J* = 7.4 Hz, 3H); 1.3 (m, 2H); 1.8 (m, 2H); 3.9 (s, 3H); 4.2 (t, *J* = 7 Hz, 2H); 6.3 (dt, *J* = 53 Hz, *J* = 6 Hz, 1H); 7.4 (s, 1H); 7.5 (s, 1H); 8.7 (s, 1H). Water mass fraction by Karl Fischer titration as synthesized was 0.0014. Anal. Calcd for C<sub>9</sub>H<sub>12</sub>F<sub>6</sub>N<sub>2</sub>O<sub>3</sub>S: C, 37.6; H, 4.7; N, 8.8. Found: C, 37.6; H, 4.6; N, 8.7.

The following mass fraction losses were observed: TGA (air): 10 % at 653.15 K, 50 % at 693.15 K. TGA (N<sub>2</sub>): 10 % at 648.15 K, 50 % at 695.15 K.

**Preparation of 1-Ethyl-3-methylimidazolium 1,1,2,2-Tetrafluoroethanesulfonate [emim][TFES].** To a 500 mL round-bottom flask was added 1-ethyl-3-methylimidazolium chloride ([emim][Cl]), 0.98 purity, Aldrich, CASRN 65039-09-0, 61.0 g, 0.416 mol) and reagent-grade acetone (500 mL). The mixture was gently warmed (323.15 K) until almost all of the [emim]-[Cl] dissolved. To a separate 500 mL flask was added potassium 1,1,2,2-tetrafluoroethanesulfonate (TFES-K, 90.2 g, 0.410 mol) along with reagent-grade acetone (350 mL). This second mixture was stirred magnetically at 297.15 K until all of the TFES-K dissolved. These solutions were combined in a 1 L flask producing a milky white suspension. The mixture was stirred at 297.15 K for 24 h. The KCl precipitate was then allowed to settle leaving a clear green solution above it. The reaction mixture was filtered once through a Celite/acetone pad and again through fritted glass to remove the KCl. The acetone was removed in vacuo first on a rotovap and then on a high vacuum

line (4 Pa, 298.15 K) for 2 h. The product was initially a viscous light yellow oil, which eventually solidified upon standing (76.0 g, 0.64 yield).

$^{19}\text{F}$  NMR (DMSO- $d_6$ )  $\delta$  [ppm]:  $-124.7$  (dt,  $J_{\text{FH}} = 6$  Hz,  $J_{\text{FF}} = 6$  Hz, 2F);  $-138.4$  (dt,  $J_{\text{FH}} = 53$  Hz, 2F).  $^1\text{H}$  NMR (DMSO- $d_6$ )  $\delta$  [ppm]: 1.3 (t,  $J = 7.3$  Hz, 3H); 3.7 (s, 3H); 4.0 (q,  $J = 7.3$  Hz, 2H); 6.1 (tt,  $J_{\text{FH}} = 53$  Hz,  $J_{\text{FH}} = 6$  Hz, 1H); 7.2 (s, 1H); 7.3 (s, 1H); 8.5 (s, 1H). Water mass fraction by Karl Fischer titration as synthesized was 0.0018. Anal. Calcd for  $\text{C}_8\text{H}_{12}\text{N}_2\text{O}_3\text{F}_4\text{S}$ : C, 32.9; H, 4.1; N, 9.6 Found: C, 33.3; H, 3.7; N, 9.6.  $M_p$  (DSC) 308.15 K.

The following mass fraction losses were observed: TGA (air): 10 % at 652.15 K, 50 % at 693.15 K. TGA ( $\text{N}_2$ ): 10 % at 651.15 K, 50 % at 691.15 K.

**Preparation of 1-Heptyl-3-methylimidazolium 1,1,2,2-Tetrafluoroethanesulfonate [hmim][TFES].** 1-Hexyl-3-methylimidazolium chloride ([hmim][Cl], 0.97 purity, Fluka, CASRN 171058-17-6, 10 g, 0.0493 mol) was mixed with reagent-grade acetone (100 mL) in a large round-bottomed flask and stirred vigorously under a nitrogen blanket. Potassium 1,1,2,2-tetrafluoroethane sulfonate (TFES-K, 10 g, 0.0455 mol) was added to reagent-grade acetone (100 mL) in a separate round-bottomed flask, and this solution was carefully added to the 1-hexyl-3-methylimidazolium chloride/acetone mixture. The mixture was left to stir overnight. The reaction mixture was then filtered using a large frit to remove the white KCl precipitate formed, and the filtrate was placed on a rotary evaporator for 4 h to remove the acetone. Final yield: 13.7 g. Appearance: pale yellow, viscous liquid at room temperature.

$^1\text{H}$  NMR (DMSO- $d_6$ ):  $\delta$  [ppm]: 0.9 (t, 3H); 1.3 (m, 6H); 1.8 (m, 2H); 3.9 (s, 3H); 4.2 (t, 2H); 6.4 (tt, 1H); 7.7 (s, 1H); 7.8 (s, 1H); 9.1 (s, 1H). Water mass fraction by Karl Fischer titration as synthesized was 0.0003.

The following mass fraction losses were observed: TGA (air): 10 % at 638.15 K, 50 % at 683.15 K. TGA ( $\text{N}_2$ ): 10 % at 643.15 K, 50 % at 688.15 K.

**Preparation of 1-Dodecyl-3-methylimidazolium 1,1,2,2-Tetrafluoroethanesulfonate [dmim][TFES].** 1-Dodecyl-3-methylimidazolium chloride ([dmim][Cl], > 0.95 purity, Acros Organics, CASRN, 114569-84-1, 34.16 g, 0.119 mol) was partially dissolved in reagent-grade acetone (400 mL) in a large round-bottomed flask and stirred vigorously. Potassium 1,1,2,2-tetrafluoroethanesulfonate (TFES-K, 26.24 g, 0.119 mol) was added to reagent-grade acetone (400 mL) in a separate round-bottomed flask, and this solution was carefully added to the 1-dodecyl-3-methylimidazolium chloride solution. The reaction mixture was heated at 333.15 K under reflux for approximately 16 h. The reaction mixture was then filtered using a large frit to remove the white KCl precipitate formed, and the filtrate was placed on a rotary evaporator for 4 h to remove the acetone. Final yield: 41.2 g.

$^{19}\text{F}$  NMR ( $\text{CD}_3\text{CN}$ ):  $\delta$  [ppm]  $-125.3$  (m, 2F);  $-137$  (dt, 2F).  $^1\text{H}$  NMR ( $\text{CD}_3\text{CN}$ ):  $\delta$  [ppm]: 0.9 (t, 3H); 1.3 (m, 18H); 1.8 (m, 2H); 3.9 (s, 3H); 4.2 (t, 2H); 6.4 (tt, 1H); 7.7 (s, 1H); 7.8 (s, 1H); 9.1 (s, 1H). Water mass fraction by Karl Fischer titration as synthesized was 0.0024.

The following mass fraction losses were observed: TGA (air): 10 % at 643.15 K, 50 % at 683.15 K. TGA ( $\text{N}_2$ ): 10 % at 648.15 K, 50 % at 683.15 K.

**Preparation of 1-Butyl-3-methylimidazolium 1,1,2,3,3,3-Hexafluoropropanesulfonate [bmim][HFPS].** 1-Butyl-3-methylimidazolium chloride ([bmim][Cl], 0.99 purity, Fluka, CASRN 79917-90-1, 50.0 g, 0.286 mol) and high-purity dry acetone (> 0.995 purity, Aldrich, 500 mL) were combined in a 1 L flask

and warmed to reflux with magnetic stirring until the solid all dissolved. At 293 K in a separate 1 L flask, potassium 1,1,2,3,3,3-hexafluoropropanesulfonate (HFPS-K) was dissolved in high-purity dry acetone (550 mL). These two solutions were combined at 293 K and allowed to stir magnetically for 12 h under positive nitrogen pressure. The stirring was stopped, and the KCl precipitate was allowed to settle. This solid was removed by suction filtration through a fritted glass funnel with a Celite pad. The acetone was removed in vacuo to give a yellow oil. The oil was further purified by diluting with high-purity acetone (100 mL) and stirring with decolorizing carbon (5 g). The mixture was suction filtered and the acetone removed in vacuo to give a colorless oil. This was further dried at 4 Pa and 298.15 K for 2 h to provide 68.6 g of product.

$^{19}\text{F}$  NMR (DMSO- $d_6$ )  $\delta$  [ppm]:  $-73.8$  (s, 3F);  $-114.5$ ,  $-121.0$  (ABq,  $J = 258$  Hz, 2F);  $-210.6$  (m, 1F,  $J = 42$  Hz).  $^1\text{H}$  NMR (DMSO- $d_6$ )  $\delta$  [ppm]: 0.9 (t,  $J = 7.4$  Hz, 3H); 1.3 (m, 2H); 1.8 (m, 2H); 3.9 (s, 3H); 4.2 (t,  $J = 7$  Hz, 2H); 5.8 (dm,  $J = 42$  Hz, 1H); 7.7 (s, 1H); 7.8 (s, 1H); 9.1 (s, 1H). Water mass fraction by Karl Fischer titration as synthesized was 0.0012. Extractable chloride by ion chromatography was 27  $\mu\text{g}/\text{mL}$ . Anal. Calcd for  $\text{C}_9\text{H}_{12}\text{F}_6\text{N}_2\text{O}_3\text{S}$ : C, 35.7; H, 4.4; N, 7.6. Found: C, 34.7; H, 3.8; N, 7.2.

The following mass fraction losses were observed: TGA (air): 10 % at 613.15 K, 50 % at 640.15 K. TGA ( $\text{N}_2$ ): 10 % at 608.15 K, 50 % at 634.15 K.

**Preparation of 1-Butyl-3-methylimidazolium 2-(1,2,2,2-Tetrafluoroethoxy)-1,1,2,2-tetrafluoroethanesulfonate [bmim][FS].** 1-Butyl-3-methylimidazolium chloride ([bmim][Cl], 0.99 purity, Fluka, CASRN 79917-90-1, 5.0 g, 0.0286 mol) was dissolved in deionized water (45 mL) at 293 K in a 100 mL flask. To this was added an aqueous solution of potassium 1,1,2,2-tetrafluoro-2-(1,2,2,2-tetrafluoroethoxy)ethanesulfonate (48.1 g of 0.20 mass fraction solution). The reaction mixture was stirred under  $\text{N}_2$  for 30 min, and the product formed as an oil layer on the bottom of the flask. The aqueous portion was decanted off, and the product layer was washed with deionized water ( $2 \times 35$  mL). The combined aqueous layers were then extracted with methylene chloride (50 mL) which was added to the product. The organic layer was dried over magnesium sulfate and the solvent was removed in vacuo first on a rotovap and then on a high vacuum line (4 Pa, 298.15 K, 6 h) to afford 8.5 g of colorless liquid (0.68 yield).

$^{19}\text{F}$  NMR ( $\text{CD}_3\text{CN}$ )  $\delta$  [ppm]:  $-83.3$ ,  $-84.1$  (subsplit ABq,  $J_{\text{FF}} = 148$  Hz, 2F);  $-83.4$  (s, 3F);  $-117.9$  (s, 2F);  $-147.1$  (dm,  $J_{\text{FH}} = 52$  Hz, 1F).  $^1\text{H}$  NMR ( $\text{CD}_3\text{CN}$ )  $\delta$  [ppm]: 0.1 (t,  $J = 7.4$  Hz, 3H); 0.5 (m, 2H); 1.0 (m, 2H); 3.0 (s, 3H); 3.4 (t,  $J = 7.2$  Hz, 2H); 6.5 (dq,  $^2J_{\text{HF}} = 52$  Hz,  $^3J_{\text{HF}} = 3$  Hz, 1H); 6.8 (s, 1H); 6.9 (s, 1H); 8.3 (s, 1H). Water mass fraction by Karl Fischer titration as synthesized was 0.0041. Extractable chloride by ion chromatography was 2.9  $\mu\text{g}/\text{mL}$ . Anal. Calcd for  $\text{C}_{12}\text{H}_{16}\text{F}_8\text{N}_2\text{O}_4\text{S}$ : C, 33.0; H, 3.7; N, 6.4. Found: C, 33.0; H, 3.4; N, 6.6.

The following mass fraction losses were observed: TGA (air): 10 % at 637.15 K, 50 % at 673.15 K. TGA ( $\text{N}_2$ ): 10 % at 643.15 K, 50 % at 680.15 K.

**Preparation of 1-Butyl-3-methylimidazolium 1,1,2-Trifluoro-2-(perfluoroethoxy)ethanesulfonate [bmim][TPES].** 1-Butyl-3-methylimidazolium chloride ([bmim][Cl], 0.99 purity, Fluka, CASRN 79917-90-1, 7.8 g, 0.0447 mol) and dry acetone (Aldrich, 150 mL) were combined at 293 K in a 500 mL flask. At 293 K in a separate 200 mL flask, potassium 1,1,2-trifluoro-2-(perfluoroethoxy)ethanesulfonate (TPES-K, 15.0 g, 0.0297 mol) was dissolved in dry acetone (300 mL). These two

**Table 4. Experimental Solubility ( $T, P, x$ ) and Diffusivity ( $D$ ) Data of R-32<sup>a</sup>**

(1) R-32 + (2) [dmpim][TMeM]				(1) R-32 + (2) [emim][BEI]			
$T$	$P$	$10^{11} D$		$T$	$P$	$10^{11} D$	
K	MPa	100 $x_1$	$m^2 \cdot s^{-1}$	K	MPa	100 $x_1$	$m^2 \cdot s^{-1}$
283.15	0.0101	1.2		283.15	0.0101	1.4	3.8
283.15	0.0996	13.6	1.4	283.15	0.1000	14.5	4.8
283.15	0.2497	31.2	2.5	283.15	0.2495	32.5	7.4
283.15	0.3997	46.0	5.0	283.15	0.3995	47.0	12
283.15	0.5495	58.6	8.9	283.15	0.5496	59.3	15
283.15	0.6997	70.0	14	283.15	0.6994	70.3	17
283.15	0.8496	80.5	16	283.15	0.8505	80.2	17
298.05	0.0100	1.0	2.7	298.15	0.0096	1.0	7.5
298.05	0.1000	9.6	2.5	298.15	0.0997	10.4	7.9
298.05	0.2496	22.6		298.15	0.2496	23.8	11
298.05	0.3996	33.7	5.5	298.15	0.3996	34.9	13
298.05	0.5493	43.5	7.9	298.15	0.5493	44.5	16
298.05	0.6995	52.0	11	298.15	0.6993	52.9	18
298.05	0.8495	59.8	13	298.15	0.8503	60.3	21
298.05	1.0000	66.7	18	298.15	1.0005	67.2	
323.15	0.0099	0.4	6.4	323.15	0.0100	0.4	
323.15	0.1000	5.7	6.7	323.15	0.0997	5.9	13
323.15	0.2494	14.1	7.9	323.15	0.2497	14.6	18
323.15	0.3995	21.5	9.6	323.15	0.3996	22.1	19
323.15	0.5495	28.1	12	323.15	0.5495	28.8	22
323.15	0.6997	34.1	13	323.15	0.6995	34.8	23
323.15	0.8494	39.7	15	323.15	0.8504	40.3	27
323.15	0.9995	44.8	17	323.15	0.9993	45.4	
348.05	0.0094	0.0		348.05	0.0101	0.1	
348.15	0.1002	3.1		348.05	0.1000	3.8	26
348.05	0.2504	8.8	12	348.05	0.2501	9.5	33
348.05	0.3996	13.9	13	348.05	0.3992	14.7	
348.05	0.5494	18.6	16	348.05	0.5496	19.6	35
348.05	0.7005	23.1		348.05	0.6996	24.1	34
348.05	0.8495	27.2		348.05	0.8504	28.3	35
348.05	1.0005	31.2	21	348.05	0.9994	32.1	

<sup>a</sup> Erratic time-dependent data: not analyzed for  $D$ .

solutions were combined and allowed to stir magnetically for 12 h under positive nitrogen pressure. The KCl precipitate was then allowed to settle leaving a colorless solution above it. The reaction mixture was filtered once through a Celite/acetone pad and again through fritted glass to remove the KCl. The acetone was removed in vacuo first on a rotovap and then on a high vacuum line (4 Pa, 298.15 K) for 2 h. Residual KCl was still precipitating out of the solution so methylene chloride (50 mL) was added to the crude product, which was then washed with deionized water (2 × 50 mL). The solution was dried over magnesium sulfate and the solvent was removed in vacuo to give the product as a viscous light yellow oil (12.0 g, 0.62 yield).

<sup>19</sup>F NMR (CD<sub>3</sub>CN)  $\delta$  [ppm]: -85.8 (s, 3F); -87.9, -90.1 (subsplit ABq,  $J_{FF} = 147$  Hz, 2F); -120.6, -122.4 (subsplit ABq,  $J_{FF} = 258$  Hz, 2F); -142.2 (dm,  $J_{FH} = 53$  Hz, 1F). <sup>1</sup>H NMR (CD<sub>3</sub>CN)  $\delta$  [ppm]: 1.0 (t,  $J = 7.4$  Hz, 3H); 1.4 (m, 2H); 1.8 (m, 2H); 3.9 (s, 3H); 4.2 (t,  $J = 7.0$  Hz, 2H); 6.5 (dm,  $J = 53$  Hz, 1H); 7.4 (s, 1H); 7.5 (s, 1H); 8.6 (s, 1H). Water mass fraction by Karl Fischer titration as synthesized was 0.00461. Anal. Calcd for C<sub>12</sub>H<sub>16</sub>F<sub>8</sub>N<sub>2</sub>O<sub>4</sub>S: C, 33.0; H, 3.7. Found: C, 32.0; H, 3.6.

The following mass fraction losses were observed: TGA (air): 10 % at 607.15 K, 50 % at 626.15 K. TGA (N<sub>2</sub>): 10 % at 603.15 K, 50 % at 638.15 K.

**Preparation of 1-Butyl-3-methylimidazolium 1,1,2-Trifluoro-2-(trifluoromethoxy)ethanesulfonate [bmim][TTES].** 1-Butyl-3-methylimidazolium chloride ([bmim][Cl], 0.99 purity, Fluka, CASRN 79917-90-1, 10.0 g, 0.0573 mol) and deionized water (15 mL) were combined at 293 K in a 200 mL flask. At 293 K in a separate 200 mL flask, potassium 1,1,2-trifluoro-2-

**Table 5. Experimental Solubility ( $T, P, x$ ) and Diffusivity ( $D$ ) Data of R-32<sup>a</sup>**

(1) R-32 + (2) [emim][BMeI]				(1) R-32 + (2) [pmpy][BMeI]			
$T$	$P$	$10^{11} D$		$T$	$P$	$10^{11} D$	
K	MPa	100 $x_1$	$m^2 \cdot s^{-1}$	K	MPa	100 $x_1$	$m^2 \cdot s^{-1}$
283.15	0.0102	1.4	4.1	283.15	0.0102	1.5	5.7
283.15	0.1001	13.6	5.1	283.15	0.1000	14.0	5.7
283.15	0.2503	30.6	8.2	283.15	0.2494	31.3	11
283.15	0.3993	44.8	13	283.15	0.3996	45.5	13
283.15	0.5493	57.0	17	283.15	0.5493	57.3	
283.15	0.7004	67.2	19	283.15	0.6996	68.3	20
283.15	0.8494	78.6		283.15	0.8495	78.2	27
298.15	0.0096	1.0	5.9	298.05	0.0095	1.0	9.9
298.15	0.0998	9.5	9.1	298.05	0.1002	9.6	10
298.15	0.2502	21.8	11	298.05	0.2503	22.2	12
298.15	0.3994	32.5	14	298.05	0.3996	33.0	15
298.15	0.5494	41.7	18	298.05	0.5497	42.2	19
298.15	0.6995	49.9	20	298.05	0.6992	50.7	22
298.15	0.8495	57.0	23	298.05	0.8496	58.0	24
298.15	0.9997	64.3		298.05	1.0004	64.5	
323.15	0.0102	0.5	15	323.15	0.0103	0.7	
323.15	0.1003	5.5	15	323.15	0.1003	5.8	19
323.15	0.2497	13.3	18	323.15	0.2498	13.8	20
323.15	0.4001	20.0	20	323.15	0.4000	20.8	
323.15	0.5495	26.4		323.15	0.5494	27.2	24
323.15	0.7003	32.0	23	323.15	0.6994	33.0	35
323.15	0.8504	36.8	30	323.15	0.8503	38.2	40
323.15	1.0004	41.7		323.15	0.9994	43.3	
348.05	0.0103	0.2		348.05	0.0103	0.3	39
348.05	0.0998	3.4	30	348.05	0.1002	3.7	39
348.05	0.2497	8.4	32	348.05	0.2502	9.0	40
348.05	0.3995	13.1	43	348.05	0.4002	13.9	40
348.05	0.5503	17.5	41	348.05	0.5493	18.4	
348.05	0.6992	21.6		348.05	0.7003	22.6	46
348.05	0.8504	25.4	48	348.05	0.8493	26.5	48
348.05	1.0005	28.8		348.05	1.0002	30.4	55

<sup>a</sup> Erratic time-dependent data: not analyzed for  $D$ .

**Table 6. Experimental Solubility ( $T, P, x$ ) and Diffusivity ( $D$ ) Data of R-32<sup>a</sup>**

(1) R-32 + (2) [bmim][TFES]				(1) R-32 + (2) [emim][TFES]			
$T$	$P$	$10^{11} D$		$T$	$P$	$10^{11} D$	
K	MPa	100 $x_1$	$m^2 \cdot s^{-1}$	K	MPa	100 $x_1$	$m^2 \cdot s^{-1}$
298.15	0.0097	0.7		298.15	0.0099	0.6	
298.15	0.0999	7.2	1.5	298.05	0.0991	5.4	
298.15	0.2500	17.2	2.7	298.05	0.2484	13.3	2.9
298.15	0.3972	26.3	4.0	298.05	0.3995	20.9	4.9
298.15	0.5484	34.5	4.8	298.05	0.5496	27.9	5.9
298.15	0.6995	42.0	7.8	298.05	0.7022	34.8	10
298.15	0.8481	49.0	8.7	298.05	0.8483	41.3	10
298.15	0.9989	55.6	14	298.05	1.0016	47.7	12

<sup>a</sup> Erratic time-dependent data: not analyzed for  $D$ .

(trifluoromethoxy)ethanesulfonate (TTES-K, 16.4 g, 0.0573 mol) was dissolved in deionized water (90 mL). These two solutions were combined at 293 K and allowed to stir magnetically for 30 min under positive nitrogen pressure to give a biphasic mixture with the desired ionic liquid as the bottom phase. The layers were separated and the aqueous phase was extracted with 2 × 50 mL portions of methylene chloride. The combined organic layers were dried over magnesium sulfate and concentrated in vacuo. The colorless oil product was dried for 4 h at 4.7 Pa and 298.15 K to afford 15.0 g of product.

<sup>19</sup>F NMR (DMSO-*d*<sub>6</sub>)  $\delta$  [ppm]: -56.8 (d,  $J_{FH} = 4$  Hz, 3F); -119.5, -119.9 (subsplit ABq,  $J = 260$  Hz, 2F); -142.2 (dm,  $J_{FH} = 53$  Hz, 1F). <sup>1</sup>H NMR (DMSO-*d*<sub>6</sub>)  $\delta$  [ppm]: 0.9 (t,  $J = 7.4$  Hz, 3H); 1.3 (m, 2H); 1.8 (m, 2H); 3.9 (s, 3H); 4.2 (t,  $J = 7.0$  Hz, 2H); 6.5 (dt,  $J = 53$  Hz,  $J = 7$  Hz, 1H); 7.7 (s, 1H);

**Table 7. Experimental Solubility ( $T, P, x$ ) and Diffusivity ( $D$ ) Data of R-32**

(1) R-32 + (2) [hmim][TFES]				(1) R-32 + (2) [dmim][TFES]			
$T$	$P$	$10^{11} D$		$T$	$P$	$10^{11} D$	
K	MPa	$100 x_1$	$m^2 \cdot s^{-1}$	K	MPa	$100 x_1$	$m^2 \cdot s^{-1}$
298.15	0.0099	0.8	3.9	298.15	0.0096	0.6	
298.15	0.1002	8.1	3.9	298.15	0.0995	7.4	4.7
298.15	0.2510	19.1	4.4	298.15	0.2510	17.9	5.1
298.15	0.3988	28.8	5.8	298.15	0.3997	27.3	3.0
298.15	0.5497	37.4	6.4	298.15	0.5481	35.7	4.7
298.15	0.6987	45.2	9.0	298.15	0.7001	43.3	6.8
298.15	0.8479	52.3	13	298.15	0.8500	50.3	8.2
298.15	0.9980	59.2	16	298.15	1.0010	56.9	13

**Table 8. Experimental Solubility ( $T, P, x$ ) and Diffusivity ( $D$ ) Data of R-32<sup>a</sup>**

(1) R-32 + (2) [dmpim][BMeI]				(1) R-32 + (2) [bmpy][BMeI]			
$T$	$P$	$10^{11} D$		$T$	$P$	$10^{11} D$	
K	MPa	$100 x_1$	$m^2 \cdot s^{-1}$	K	MPa	$100 x_1$	$m^2 \cdot s^{-1}$
298.05	0.0099	0.8	6.3	298.15	0.0096	1.0	6.8
298.15	0.0995	9.0	6.6	298.15	0.0995	10.0	7.8
298.15	0.2495	21.3	8.9	298.15	0.2495	22.4	12
298.15	0.3976	31.9	12	298.15	0.3995	33.1	15
298.15	0.5501	41.5	15	298.15	0.5496	42.8	15
298.15	0.7017	50.1	18	298.15	0.7005	51.0	
298.15	0.8513	57.8	22	298.15	0.8506	58.6	
298.15	1.0011	65.1	23	298.15	1.0000	65.4	23

<sup>a</sup> Erratic time-dependent data: not analyzed for  $D$ .**Table 9. Experimental Solubility ( $T, P, x$ ) and Diffusivity ( $D$ ) Data of R-32<sup>a</sup>**

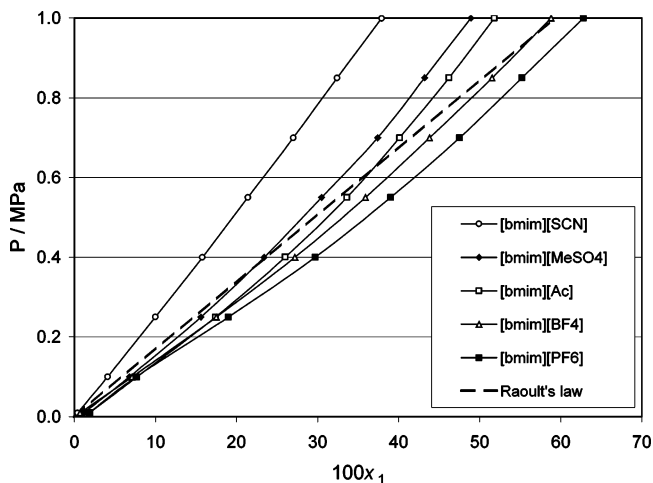
(1) R-32 + (2) [bmim][Ac]				(1) R-32 + (2) [bmim][SCN]			
$T$	$P$	$10^{11} D$		$T$	$P$	$10^{11} D$	
K	MPa	$100 x_1$	$m^2 \cdot s^{-1}$	K	MPa	$100 x_1$	$m^2 \cdot s^{-1}$
298.25	0.0099	1.0	2.2	298.15	0.0095	0.4	8.1
298.15	0.0997	7.7	2.6	298.15	0.1003	4.1	8.6
298.15	0.2498	17.4	4.1	298.15	0.2503	10.0	10
298.15	0.4004	26.0	5.6	298.15	0.3996	15.8	11
298.15	0.5498	33.6	10	298.15	0.5500	21.4	
298.15	0.6997	40.1	15	298.15	0.6997	27.0	14
298.05	0.8502	46.2	18	298.15	0.8495	32.4	18
298.15	1.0004	51.8	21	298.15	0.9992	37.9	21

<sup>a</sup> Erratic time-dependent data: not analyzed for  $D$ .**Table 10. Experimental Solubility ( $T, P, x$ ) and Diffusivity ( $D$ ) Data of R-32**

(1) R-32 + (2) [bmim][MeSO <sub>4</sub> ]				(1) R-32 + (2) [bmim][HFPS]			
$T$	$P$	$10^{11} D$		$T$	$P$	$10^{11} D$	
K	MPa	$100 x_1$	$m^2 \cdot s^{-1}$	K	MPa	$100 x_1$	$m^2 \cdot s^{-1}$
298.15	0.0099	1.2	2.1	298.15	0.0095	1.0	3.3
298.15	0.1001	6.8	2.7	298.15	0.1000	10.4	3.2
298.15	0.2498	15.6	3.0	298.15	0.2498	24.2	3.9
298.15	0.3995	23.4	4.2	298.15	0.3995	35.0	7.0
298.25	0.5501	30.5	5.2	298.15	0.5495	44.6	7.0
298.15	0.6995	37.4	6.2	298.15	0.6998	52.7	11
298.15	0.8500	43.2	9.9	298.15	0.8494	60.4	10
298.15	1.0006	48.9	12	298.15	1.0004	67.0	17

7.8 (s, 1H); 9.1 (s, 1H). Water mass fraction by Karl Fischer titration as synthesized was 0.00061. Extractable chloride by ion chromatography was  $< 2 \mu\text{g/mL}$ . Anal. Calcd for  $\text{C}_{11}\text{H}_{16}\text{F}_6\text{N}_2\text{O}_4\text{S}$ : C, 34.2; H, 4.2; N, 7.3. Found: C, 34.0; H, 4.0; N, 7.1.

The following mass fraction losses were observed: TGA (air): 10 % at 601.15 K, 50 % at 627.15 K. TGA ( $\text{N}_2$ ): 10 % at 597.15 K, 50 % at 624.15 K.

**Figure 1.** Isothermal  $Px$  (solubility) diagram for R-32 + [bmim][PF<sub>6</sub>],<sup>12</sup> R-32 + [bmim][BF<sub>4</sub>],<sup>12</sup> R-32 + [bmim][Ac], R-32 + [bmim][SCN], and R-32 + [bmim][MeSO<sub>4</sub>] mixtures at 298.15 K. Solid lines: NRTL model. Symbols: present experimental data.**Table 11. Experimental Solubility ( $T, P, x$ ) and Diffusivity ( $D$ ) Data of R-32<sup>a</sup>**

(1) R-32 + (2) [bmim][FS]				(1) R-32 + (2) [bmim][TPES]			
$T$	$P$	$10^{11} D$		$T$	$P$	$10^{11} D$	
K	MPa	$100 x_1$	$m^2 \cdot s^{-1}$	K	MPa	$100 x_1$	$m^2 \cdot s^{-1}$
298.15	0.0100	0.9	4.3	298.15	0.0095	1.0	4.5
298.15	0.0997	9.2	4.3	298.15	0.1001	10.2	5.3
298.15	0.2501	21.4	5.4	298.15	0.2496	23.7	6.7
298.15	0.4004	31.9	9.1	298.15	0.3995	34.8	9.6
298.15	0.5500	41.5	10	298.15	0.5494	44.5	12
298.15	0.6996	49.7	15	298.15	0.6994	52.9	15
298.15	0.8494	57.1		298.15	0.8495	60.5	18
298.15	1.0005	63.8	28	298.15	0.9994	67.4	21

<sup>a</sup> Erratic time-dependent data: not analyzed for  $D$ .**Table 12. Experimental Solubility ( $T, P, x$ ) and Diffusivity ( $D$ ) Data of R-32**

(1) R-32 + (2) [bmim][TTES]							
$T$	$P$	$10^{11} D$		$T$	$P$	$10^{11} D$	
K	MPa	$100 x_1$	$m^2 \cdot s^{-1}$	K	MPa	$100 x_1$	$m^2 \cdot s^{-1}$
298.15	0.0095	1.0	4.3	298.15	0.5500	42.8	10
298.15	0.1003	9.6	4.5	298.15	0.6997	51.0	12
298.15	0.2503	22.3	5.8	298.15	0.8495	58.3	16
298.15	0.3996	33.4	7.1	298.15	0.9992	65.0	25

## Results

The present solubility [VLE ( $T, P, x$ )] data are summarized in Tables 4 to 12. Figures 1 to 4 show plots of molar compositions versus pressure at 298.15 K (dashed line represents Raoult's law). Interestingly large differences in the solubility of R-32 in RTILs with and without fluorinated anions are clearly observed in Figure 1.

Diffusivity ( $D$ ) was obtained from the analysis of time-dependent absorption data,  $\langle C \rangle$ , using the following model equation:<sup>15,21</sup>

$$\langle C \rangle = C_s \left[ 1 - 2 \left( 1 - \frac{C_0}{C_s} \right) \sum_{n=0}^{\infty} \frac{\exp(-\lambda_n^2 D t)}{L^2 \lambda_n^2} \right] \quad (1)$$

where  $\langle C \rangle$  is the space-averaged concentration;  $C_0$  and  $C_s$  are the initial and final concentrations of a solution mixture, respectively;  $\lambda_n = (n + 1/2)\pi/L$  is the eigenvalue; and  $L$  is the liquid depth of the solution in a test container. Detail procedures



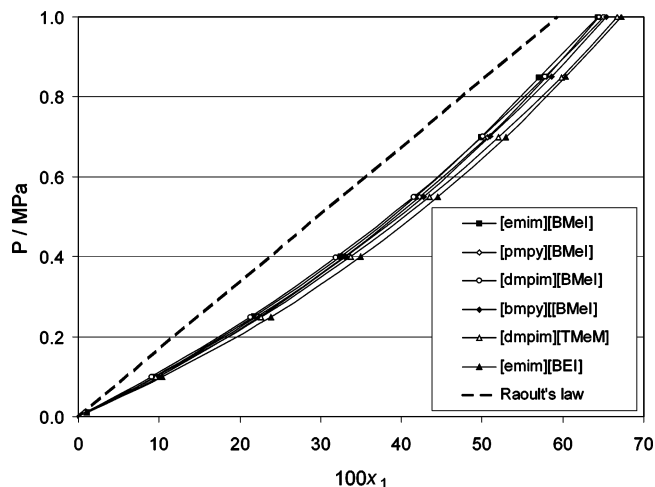


**Figure 2.** Isothermal  $Px$  (solubility) diagram for R-32 + [dmpim][TMeM], R-32 + [emim][BEI], R-32 + [pmpy][BMeI], R-32 + [emim][BMeI], R-32 + [dmpim][BMeI], and R-32 + [bpy][BMeI] mixtures at 298.15 K. Solid lines: NRTL model. Symbols: present experimental data.

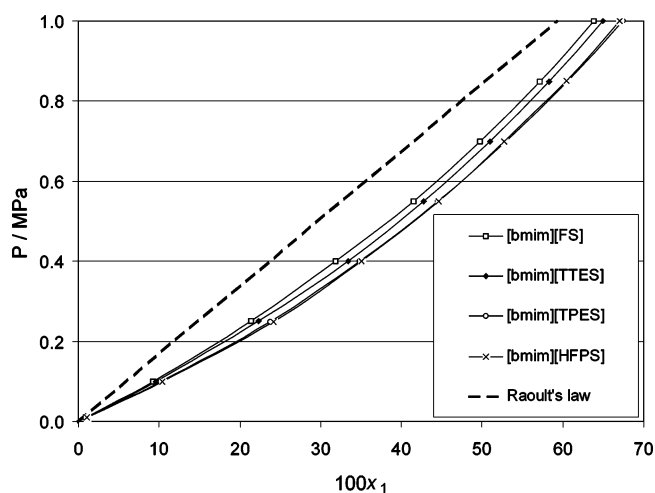


**Figure 3.** Isothermal  $Px$  (solubility) diagram for R-32 + [bmim][HFPS], R-32 + [bmim][TPES], R-32 + [bmim][TTES], and R-32 + [bmim][FS] mixtures at 298.15 K. Solid lines: NRTL model. Symbols: present experimental data.

of the analysis are given in our previous work.<sup>15</sup> The results are shown in Tables 4 to 12, together with the solubility ( $T$ ,  $P$ ,  $x$ ) data.

### Data Correlation

In this section, we analyze the experimental solubility ( $T$ ,  $P$ ,  $x$ ) data with the existing solution models for nonelectrolyte solutions, which may also be applied even for electrolyte solutions.<sup>22–25</sup>

**Solubility Model.** In general, low- and medium-pressure vapor liquid equilibria (VLE) for an  $N$ -component system can be described by:<sup>26</sup>

$$y_i P \Phi_i = x_i \gamma_i P_i^s, \quad (i = 1, \dots, N) \quad (2)$$

where  $y_i$  is the vapor phase mol fraction for  $i$ th species,  $x_i$  is the liquid-phase mol fraction for  $i$ th species,  $P$  is pressure,  $P_i^s$  is the saturated vapor pressure for  $i$ th species,  $\Phi_i$  is a correction factor for  $i$ th species ( $= 1$  at sufficiently low pressures), and  $\gamma_i$  is the activity coefficient for  $i$ th species (function of compositions at  $T$ ). For a binary system ( $N = 2$ ) of gas (1) + ionic

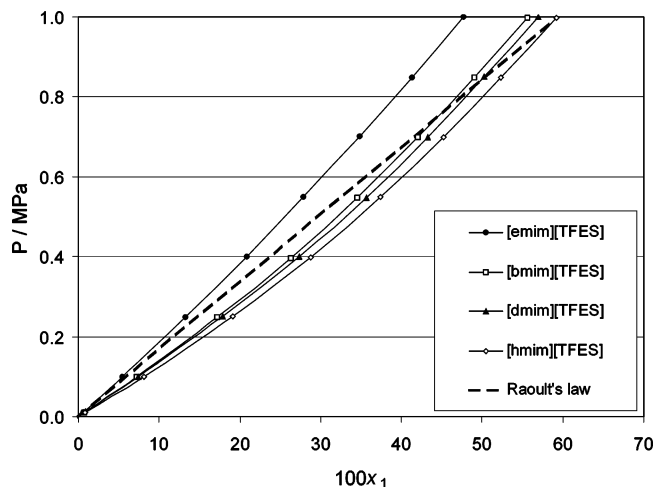


**Figure 4.** Isothermal  $Px$  (solubility) diagram for R-32 + [bmim][TFES], R-32 + [emim][TFES], R-32 + [hmim][TFES], and R-32 + [dmim][TFES] mixtures at 298.15 K. Solid lines: NRTL model. Symbols: present experimental data.

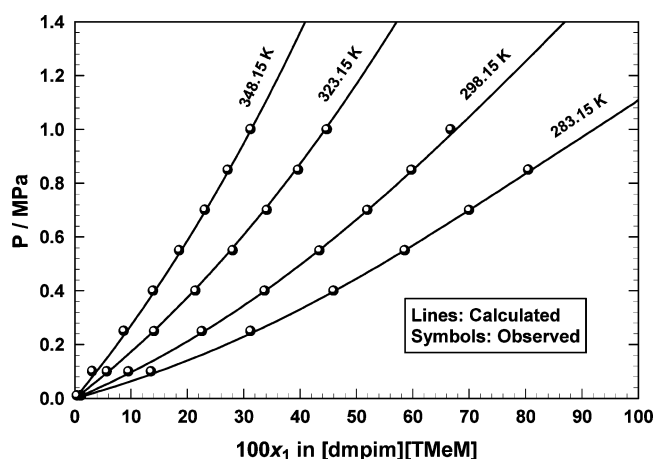


**Figure 5.** Isothermal  $Px$  (solubility) diagram for R-32 + [dmpim][TMeM]. Lines: NRTL model calculations. Symbols: present experimental data.

liquid (2) mixtures, it is reasonable to assume that  $y_1 = 1$  (or  $y_2 = 0$ ) at the present temperatures of interest; i.e.,  $P_2^s \approx 0$ . The activity coefficient for species 1 is given by

$$\gamma_1 = \frac{P \Phi_1}{x_1 P_1^s} \quad (3)$$

The correction factor  $\Phi_1$  for the present case is<sup>26</sup>

$$\Phi_1 = \exp \left[ \frac{(B_1 - \bar{V}_1)(P - P_1^s)}{RT} \right] \quad (4)$$

where the 2nd virial coefficient of species 1 is  $B_1(T)$ , which was obtained by an equation of state (EOS) computer program.<sup>15,27</sup> Similarly the molar volume,  $\bar{V}_1$ , can be calculated if  $T$  is less than the critical point  $T_c$  of a pure component 1. However, as presented in our previous work,<sup>12</sup> we adopt an approximate  $\bar{V}_1$ , which is defined by eq 5, and can be applied even for temperatures above  $T_c$ :

$$\bar{V}_1 = (1 - \alpha_v) \bar{V}_2 \quad (5)$$

$\bar{V}_2$  is a molar liquid volume of ionic liquid at  $T$ , and  $\alpha_v$  is a unique temperature-independent constant.

**Table 13. Determined Parameters for the NRTL Activity-Coefficient Model**

system (1) + (2)	$\tau_{12}^{(0)}$	$\tau_{12}^{(1)}$		$\tau_{21}^{(1)}$		$\Delta P$
		K	$\tau_{21}^{(0)}$	K	MPa <sup>a</sup>	
R-32 + [bmim][PF <sub>6</sub> ] <sup>b</sup>	4.408	-565.89	-1.0275	-199.06	0.0067	
R-32 + [bmim][BF <sub>4</sub> ] <sup>b</sup>	0.6154	714.11	0.5525	-674.40	0.0078	
R-32 + [dmpim][TMeM] <sup>c</sup>	0	735.88	0	-558.92	0.0071	
R-32 + [emim][BEI] <sup>c</sup>	0	837.22	0	-621.72	0.0058	
R-32 + [emim][BMeI] <sup>c</sup>	0	959.31	0	-621.18	0.0047	
R-32 + [pmpy][BMeI] <sup>c</sup>	0	987.57	0	-645.97	0.0063	

<sup>a</sup> Standard deviations in pressure of the nonlinear regression analysis with  $\alpha = 0.2$ . <sup>b</sup> Ref 12. <sup>c</sup> In this work,  $\alpha_v = 0.75$ .

For RTILs,  $\bar{V}_2$  is given by

$$\bar{V}_2[\text{cm}^3/\text{mol}] = \frac{M_2}{\rho_2} \quad (6)$$

where  $M_2$  is the ionic liquid molecular weight. Coefficients in  $\rho_2$ , the ionic liquid density, were obtained by fitting experimental liquid densities of RTILs<sup>15</sup> shown in Table 2. Concerning the vapor pressure of pure species 1 ( $P_1^s$ ), we use an Antoine type equation similar to our previous report.<sup>12</sup> For difluoromethane,  $A_1 = 9.49117$ ,  $B_1 = 3006.86$ , and  $C_1 = 37.1416$  between 283.15 K and 348.15 K:  $\ln(P_1^s/\text{MPa}) = A_1 - B_1/(T/\text{K} + C_1)$ .

For each solubility data, the activity coefficients  $\gamma_1$  were calculated at each observed  $x_1$  point. Several activity models are available in the literature.<sup>28,29</sup> In this work, like our previous work,<sup>12</sup> we chose the nonrandom two-liquid (NRTL) equations:

$$\ln \gamma_1 = x_2^2 \left[ \tau_{21} \left( \frac{G_{21}}{x_1 + x_2 G_{21}} \right)^2 + \frac{\tau_{12} G_{12}}{(x_2 + x_1 G_{12})^2} \right] \quad (7)$$

$$\ln \gamma_2 = x_1^2 \left[ \tau_{12} \left( \frac{G_{12}}{x_2 + x_1 G_{12}} \right)^2 + \frac{\tau_{21} G_{21}}{(x_1 + x_2 G_{21})^2} \right] \quad (8)$$

where  $G_{12}$  and  $G_{21}$  are defined by three NRTL interaction parameters ( $\tau_{12}$ ,  $\tau_{21}$ ,  $\alpha$ ):

$$G_{12} \equiv \exp(-\alpha\tau_{12}) \text{ and } G_{21} \equiv \exp(-\alpha\tau_{21}) \quad (9)$$

where  $\alpha = 0.2$  (assumed to be a constant of 0.2 in this work).

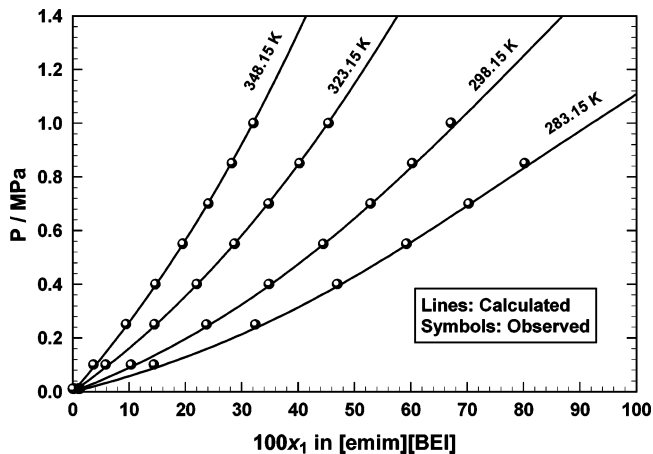
In this study, we have modeled  $\tau_{12}$  and  $\tau_{21}$  (adjustable binary interaction parameters) using only the temperature-dependent terms ( $\tau_{12}^{(1)}$ ,  $\tau_{21}^{(1)}$ ) as shown in eq 10:

$$\tau_{12} = \tau_{12}^{(0)} + \tau_{12}^{(1)}/T \text{ and } \tau_{21} = \tau_{21}^{(0)} + \tau_{21}^{(1)}/T \quad (10)$$

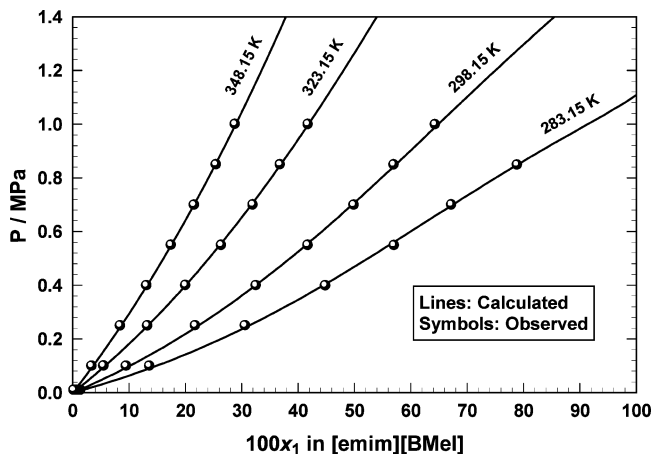
The binary interaction parameters were obtained using the same procedure as described in our previous paper<sup>12</sup> with a standard deviation in the pressure fit of (0.005 to 0.008) MPa.

Figure 5 shows an example for the comparison of isothermal  $Px$  plots using the R-32 + [dmpim][TMeM] system. The binary interaction parameters used in Figure 5 are  $\tau_{12}^{(1)} = 735.88$  K and  $\tau_{21}^{(1)} = -558.92$  K in eq 10, respectively. Standard deviations in the pressure fit are 0.0071 MPa. All observed solubility behaviors in the present ionic solutions have been well-correlated using this method. Determined binary interaction parameters in eq 10 are listed in Table 13 for the present binary systems. Selected isothermal  $Px$  diagrams calculated with these parameters are compared with observed values in Figures 5 to 8.

**Diffusivity Model.** A semi-theoretical model for correlating the diffusivity data based on the Einstein–Stokes equation<sup>29,30</sup>



**Figure 6.** Isothermal  $Px$  (solubility) diagrams for R-32 + [emim][BEI]. Lines: NRTL model calculations. Symbols: present experimental data.



**Figure 7.** Isothermal  $Px$  (solubility) diagrams for R-32 + [emim][BMeI]. Lines: NRTL model calculations. Symbols: present experimental data.

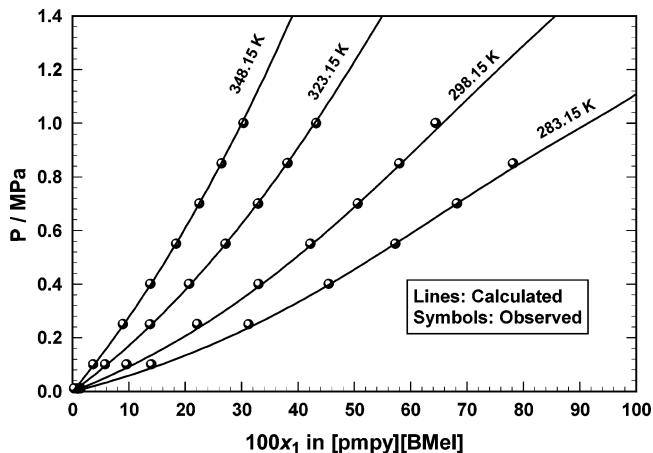


**Figure 8.** Isothermal  $Px$  (solubility) diagrams for R-32 + [pmpy][BMeI]. Lines: NRTL model calculations. Symbols: present experimental data.

was developed in our previous work:<sup>12</sup>

$$D = \frac{kT}{6\pi r \eta_0 (\eta/\eta_0)^b} \quad (11)$$

or

$$\ln[(D/\text{m}^2 \cdot \text{s}^{-1})/(T/\text{K})] = a - b \ln(\eta/\eta_0) \quad (12)$$

where  $a = \ln(k/6\pi r \eta_0)$  and  $b$  are adjustable parameters,  $k$  is

**Table 14. Coefficients in Equation 15<sup>a</sup>**

compound <i>i</i>	$A_i$	$B_i/K$	$C_i/K^{-1}$	$D_i/K^{-2}$
R-32 <sup>b</sup>	4.738618	-461.5	$-1.80359 \times 10^{-2}$	0
[bmim][PF <sub>6</sub> ] <sup>c</sup>	-182.774	24992.4	$4.84019 \times 10^{-1}$	$-4.44779 \times 10^{-4}$
[bmim][BF <sub>4</sub> ] <sup>c</sup>	-149.99	20757.8	$3.91576 \times 10^{-1}$	$-3.55363 \times 10^{-4}$
[dmpim][TMeM]	-453.339	55763.2	1.28183	$-1.23045 \times 10^{-3}$
[emim][BEI]	-132.704	18418.7	$3.47097 \times 10^{-1}$	$-3.16469 \times 10^{-4}$
[emim][BMeI]	-131.216	16999.1	$3.64551 \times 10^{-1}$	$-3.49193 \times 10^{-4}$
[pmpy][BMeI]	-106.941	15665.9	$2.63777 \times 10^{-1}$	$-2.26912 \times 10^{-4}$

<sup>a</sup> Viscosity in mPa·s (or cP), and *T* in K (for ionic liquids: 283 < *T* < 373 K). <sup>b</sup> Ref 37. <sup>c</sup> New measurement using capillary viscometer, replaces data in ref 12.

**Table 15. Determined Parameters in Equations 12 and 13**

system	$a/\ln \text{m}^2 \cdot \text{s}^{-1} \cdot \text{K}^{-1}$	$b/\ln \text{m}^2 \cdot \text{s}^{-1} \cdot \text{K}^{-1}$	<i>c</i>	<i>r</i> /nm
R-32 + [bmim][PF <sub>6</sub> ] <sup>a</sup>	$-27.452 \pm 0.106$	$0.474 \pm 0.026$	0.5	$0.61 \pm 0.06$
R-32 + [bmim][BF <sub>4</sub> ] <sup>a</sup>	$-27.229 \pm 0.109$	$0.560 \pm 0.032$	0.5	$0.49 \pm 0.05$
R-32 + [dmpim][TMeM]	$-26.679 \pm 0.093$	$0.524 \pm 0.021$	0.4	$0.28 \pm 0.03$
R-32 + [emim][BEI]	$-26.220 \pm 0.096$	$0.636 \pm 0.0288$	1.0	$0.18 \pm 0.02$
R-32 + [emim][BMeI]	$-25.809 \pm 0.137$	$0.927 \pm 0.0505$	0.7	$0.12 \pm 0.02$
R-32 + [pmpy][BMeI]	$-26.110 \pm 0.109$	$0.643 \pm 0.0352$	0.7	$0.16 \pm 0.02$

<sup>a</sup> Based on solubility data from ref 12 and viscosity data in this work.

Boltzmann constant, *r* is the radius, and  $\eta_0$  is a unit viscosity (1 mPa·s) that is needed as a normalization factor for the equation to have the proper dimension. Concerning the solution viscosity in eq 12, we adopt our earlier model for an *N*-component solution viscosity:<sup>31</sup>

$$\ln(\eta/\eta_0) = \sum_{i=1}^N \xi_i \ln(\eta_i/\eta_0) \quad (13)$$

where

$$\xi_i = M_i^c x_i / \sum_{i=1}^N M_i^c x_i \quad (14)$$

and  $M_i$  is the molecular weight of the *i*th species. The present diffusivity model, eq 12 with eqs 13 and 14, has three empirical adjustable parameters (*a*, *b*, and *c*) to correlate observed diffusivity data (function of *x* and *T*), provided that the viscosity of each pure species is known. The dynamic viscosity of a pure compound *i* is modeled as:

$$\ln(\eta_i/\text{mPa}\cdot\text{s}) = A_i + \frac{B_i}{(T/K)} + C_i(T/K) + D_i(T/K)^2 \quad (15)$$

Coefficients in eq 15 for several compounds studied here are given in Table 14.

Similar to our previous analysis,<sup>12</sup> a linear regression analysis was applied to obtain the parameters *a* and *b* with a fixed value for *c*. Determined parameters for six systems are listed in Table 15. The molecular radius for R-32 is calculated from the *a* parameter in eq 12, which can be rearranged  $r = k/(6\pi\eta_0 \exp a)$ . The model calculations with these parameters are compared with experimental diffusivity data in Figures 9 to 12. The model calculation is in good agreement with the experimental data with an overall error of less than 10 % (largest single error of 20 %).

## Discussion

In this work, we have conducted a systematic study of the solubility of R-32 with a variety of RTILs having both fluorinated and nonfluorinated anions. The fluorinated anions included a methide ([TMeM]), two imides ([BMeI] and [BEI]), and five newly synthesized sulfonates ([TFES], [HFPS], [FS],

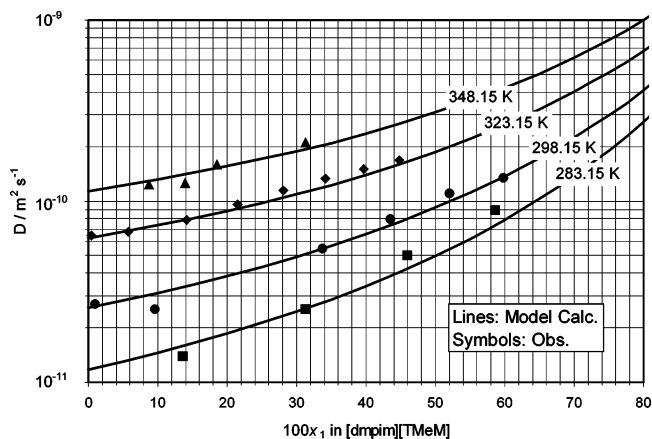


**Figure 9.** Diffusivity versus composition diagram of R-32 in [dmpim]-[TMeM]. Lines: model calculations (see text). Symbols: present experimental data.

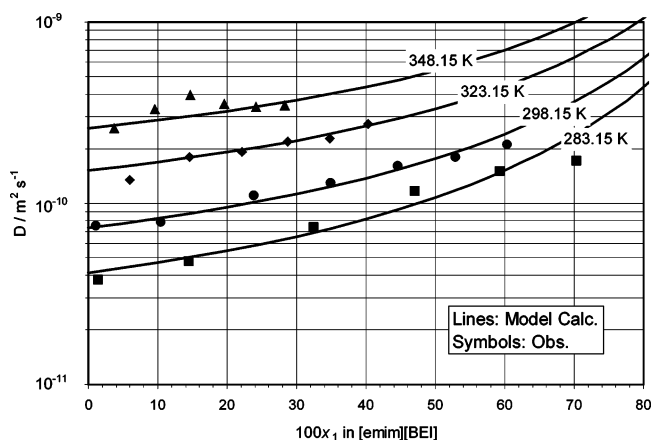


**Figure 10.** Diffusivity versus composition diagram of R-32 in [emim]-[BEI]. Lines: model calculations (see text). Symbols: present experimental data.

[TPES], [TTES]). Nonfluorinated anions included acetate ([Ac]), thiocyanate ([SCN]), and methyl sulfate ([MeSO<sub>4</sub>]). All cations were based on imidazolium, except [bmpy], which was based on pyridinium. The thermal stability of the synthesized RTILs was measured by TGA. The synthesized RTILs were found to be thermally stable by measuring the mass fraction loss during

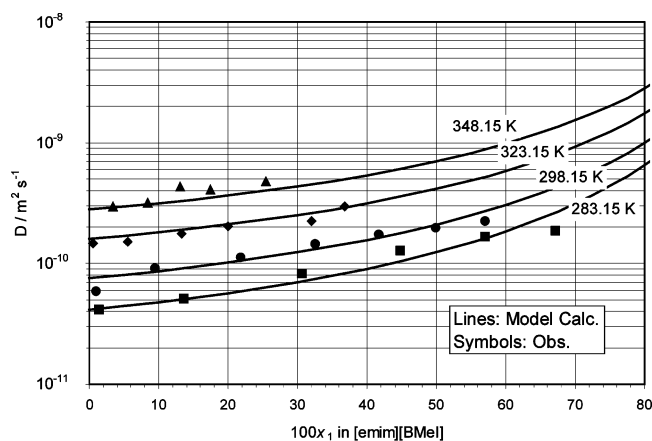


**Figure 11.** Diffusivity versus composition diagram of R-32 in [emim]-[BMeI]. Lines: model calculations (see text). Symbols: present experimental data.

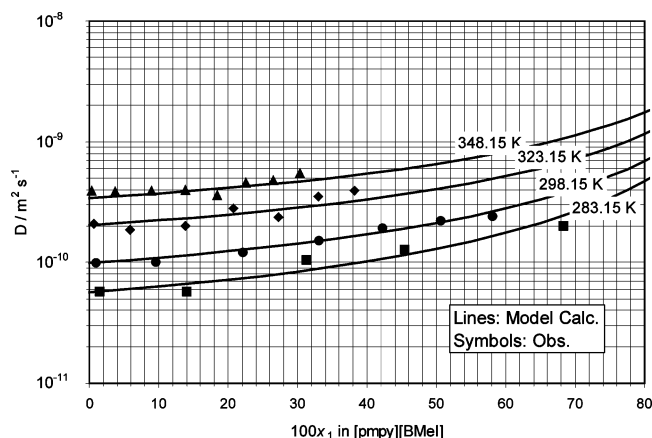


**Figure 12.** Diffusivity versus composition diagram of R-32 in [pmpy]-[BMeI]. Lines: model calculations (see text). Symbols: present experimental data.

heating in air (601 K to 653 K at 10 % loss and 627 K to 693 K at 50 % loss) and nitrogen (597 K to 648 K at 10 % loss and 624 K to 695 K at 50 % loss). The most thermally stable RTIL was [TFES]. The order of thermal stability was [TFES] > [FS] > [HFPS] > [TPES] > [TTES]. The trend in thermal stability between the potassium salts and the [bmim] salts was the same and clearly dominated by the anion.

A comparison between the solubility of R-32 in the 19 RTILs was made at 298.15 K and 0.6 MPa in Figures 1 to 4. In general, the fluorinated anions (except [emim][TFES]) have significant higher mole fraction solubility (0.37 to 0.47) in R-32 than the nonfluorinated anions (0.23 to 0.36) at 298 K, see Figure 1. Raoult's law is plotted on the same Figures 1 to 4 to obtain a measure of the nonideality (positive and negative deviation behavior). Isotherms above the Raoult's law line indicate positive deviation behavior between R-32 and the ionic liquid (i.e., low solubility). Isotherms below the Raoult's law line indicate negative deviation behavior between R-32 and the ionic liquid (i.e., high solubility). The three RTILs with the highest attraction for R-32 were [bmim][HFPS], [bmim][TPES], and [emim][BEI] (see Figures 2 and 3). A comparison between the five sulfonate anions with a common [bmim] cation show the highest to lowest negative deviation behavior between R-32 and the anions was [HFPS] > [TPES] > [TTES] > [FS] > [TFES] (see Figure 3). Although it may not be possible to separate the affect of the anion and cation into individual positive and negative deviation behavior with R-32, the cation in some cases

also appears to play a significant role when determining the solubility of R-32 in the ionic liquids. For example, for the case where the [TFES] anion remains the same the order of attraction between R-32 and the cations was [hmim] > [dmim] > [bmim] > [emim] (see Figure 4). In fact, the [emim][TFES] actually shows positive deviation behavior rather than negative deviation behavior; therefore, the size of the cation may also play an important role when optimizing the storage of R-32 molecules. Another example, where the cation had a much smaller affect with the common imide [BMeI] anion was [bmpy]  $\approx$  [dmpim]  $\approx$  [emim]  $\approx$  [pmpy] (see Figure 2). Preliminary ab initio molecular simulations indicate that H-bonding (H-F) between both fluorine on the anion and hydrogen on R-32 as well as fluorine on R-32 and hydrogen on the cation are contributing to attractions (i.e., high solubility). A clear understanding of this behavior can be used for designing new fluorinated ionic liquids in the future.

All solubility (VLE) data of the present binary systems with RTILs have been successfully correlated with the conventional activity models for nonelectrolyte solutions. However, as mentioned in our previous work,<sup>12</sup> the present results are not surprising since several successful attempts using nonelectrolyte models for electrolyte solutions are known in the literature.<sup>22–25</sup> Finally, the observed diffusivity behaviors ( $D$  vs  $x$  plots) have been well-explained by a simple diffusion model, developed in our previous study.<sup>12</sup> The model is based on the theoretical Stokes–Einstein model plus a well-known empirical relation between solution viscosity and diffusivity. As discussed in the diffusivity modeling section, the empirical fitting parameter,  $a$  in eq 12, may contain a physically meaningful quantity (i.e., the size of the diffusing body). In the case of R-32 in the ionic liquids, the present model provided a molecular size derived diffusing body size from about 1 (in [emim][BEI], [emim]-[BMeI], [pmpy][BMeI]) to 2 to 3 (in [dmpim][TMeM], [bmim]-[BF<sub>4</sub>], [bmim][PF<sub>6</sub>]) times larger than the known size of R-32 ( $r = d/2 = 0.1784$  nm).<sup>32</sup> As mentioned in our previous study, it is intriguing to imagine that R-32 diffuses in the RTILs as clusters (or molecular associations).<sup>12</sup> Our previous estimates (5 to 8 times the known size) for the derived diffusing body size of R-32 in [bmim][BF<sub>4</sub>] and [bmim][PF<sub>6</sub>] may be overestimated due to the original viscosity data being too low. FT-IR experiments are underway to prove whether clustering (i.e., the formation of dimers or trimers) may be occurring. Previous studies have shown that this affect does occur in H-bonding solutions (alcohols in hydrocarbon solvents) and can be measured using FT-IR.<sup>33–36</sup>

## Conclusions

New experimental results for the solubility and diffusivity of R-32 in 19 RTILs are presented for temperatures from 283.15 K to 348.15 K and pressures up to 1.0 MPa. Eight of these RTILs were synthesized for the first time with five new fluorinated sulfonate anions ([TFES], [HFPS], [TPES], [TTES], and [FS]). We have found that large solubility differences exist between ionic liquids with fluorinated anions (high solubility for R-32) and nonfluorinated anions (lower solubility for R-32). RTILs with fluorinated anions with the strongest attraction for R-32 were [bmim][HFPS], [bmim][TPES], and [emim][BEI]. Although the mechanism of the solubility difference is not clear in an intermolecular level, hydrogen bonding is believed to play an important role between the two R-32 hydrogens and the multiple anion fluorines as well as the two R-32 fluorines and the multiple cation hydrogens. The design of new RTILs with fluorinated anions (particularly fluorinated C<sub>x</sub>F<sub>y</sub>H<sub>z</sub>-sulfonates,

bis(C<sub>x</sub>F<sub>y</sub>H<sub>z</sub>-sulfonyl)imides, and tris(C<sub>x</sub>F<sub>y</sub>H<sub>z</sub>-sulfonyl)methides with fluorinated and nonfluorinated cations will be explored further.

The observed VLE (*P*, *T*, *x*) behaviors of ionic liquids with R-32 have been well-correlated with the conventional solution (activity coefficient) models for nonelectrolyte solutions. The observed behaviors of the isothermal diffusivity in the pressure or composition space have been successfully correlated with a semi-theoretical model. Derived molecular size of the R-32 diffusing body suggests that the formation of dimers and trimers (clustering) of R-32 molecules maybe occurring in RTILs such as [bmim][PF<sub>6</sub>], [bmim][BF<sub>4</sub>], and [dmpim][TMeM].

### Acknowledgment

The authors thank Mr. Brian L. Wells for conducting the microbalance experiments and Mr. Seun S. Solesi for his assistance in calculating the diffusivity data. We also thank Dr. Richard A. Maynard, Linda M. Williams, and Michael J. Logue for making the density, viscosity, and water titration measurements, respectively.

### Literature Cited

- Pérez-Salado Kamps, Á.; Tuma, D.; Xia, J.; Maurer, G. Solubility of CO<sub>2</sub> in the ionic liquid [bmim][PF<sub>6</sub>]. *J. Chem. Eng. Data* **2003**, *48*, 746–749.
- Kumelan, J.; Pérez-Salado Kamps, Á.; Tuma, D.; Maurer, G. Solubility of CO in the ionic liquid [bmim][PF<sub>6</sub>]. *Fluid Phase Equilib.* **2005**, *228–229*, 207–211.
- Cadena, C.; Anthony, J. L.; Shah, J. K.; Morrow, T. I.; Brennecke, J. F.; Maginn, E. J. Why is CO<sub>2</sub> so soluble in imidazolium-based ionic liquids? *J. Am. Chem. Soc.* **2004**, *126*, 5300–5308.
- Husson-Borg, P.; Majer, V.; Costa Gomes, M. F. Solubilities of oxygen and carbon dioxide in butyl methyl imidazolium tetrafluoroborate as a function of temperature and at pressures close to atmospheric pressure. *J. Chem. Eng. Data* **2003**, *48*, 480–485.
- Anthony, J. L.; Maginn, E. J.; Brennecke, J. F. Solubilities and thermodynamic properties of gases in the ionic liquid 1-*n*-butyl-3-methylimidazolium hexafluorophosphate. *J. Phys. Chem. B* **2002**, *106*, 7315–7320.
- Camper, D.; Scovazzo, P.; Koval, C.; Noble, R. Gas solubilities in room-temperature ionic liquids. *Ind. Eng. Chem. Res.* **2004**, *43*, 3049–3054.
- Morgan, D.; Ferguson, L.; Scovazzo, P. Diffusivities of gases in room-temperature ionic liquids: data and correlations obtained using a lag-time technique. *Ind. Eng. Chem. Res.* **2005**, *44*, 4815–4823.
- Shariati, A.; Gutkowski, K.; Peters, C. J. Comparison of the phase behavior of some selected binary systems with ionic liquids. *AIChE J.* **2005**, *51* (5), 1532–1540.
- Shariati, A.; Peters, C. J. High-pressure phase behavior of systems with ionic liquids: measurements and modeling of the binary system fluoroform + 1-ethyl-3-methylimidazolium hexafluorophosphate. *J. Supercrit. Fluids* **2003**, *25*, 109–117.
- Shariati, A.; Peters, C. J. High-pressure phase behavior of systems with ionic liquids. II. The binary system carbon dioxide + 1-ethyl-3-methylimidazolium hexafluorophosphate. *J. Supercrit. Fluids* **2004**, *29*, 43–48.
- Shariati, A.; Peters, C. J. High-pressure phase behavior of systems with ionic liquids. Part III. The binary system carbon dioxide + 1-hexyl-3-methylimidazolium hexafluorophosphate. *J. Supercrit. Fluids* **2003**, *30*, 139–144.
- Shiflett, M. B.; Yokozeki, A. Solubilities and diffusivities of hydrofluorocarbons in room-temperature ionic liquids. *AIChE J.* (in press).
- Abbott, A. P.; Eardley, C. A.; Harper, C. J.; Hope, G. E. Electrochemical investigations in liquid and supercritical 1,1,1,2-tetrafluoroethane (HFC 134a) and difluoromethane (HFC 32). *J. Electroanal. Chem.* **1998**, *457*, 1–4.
- Abbott, A. P.; Eardley, C. A. Conductivity of (C<sub>4</sub>H<sub>9</sub>)<sub>4</sub>N BF<sub>4</sub> in liquid and supercritical hydrofluorocarbons. *J. Phys. Chem. B* **2000**, *104*, 9351–9355.
- Shiflett, M. B.; Yokozeki, A. Solubilities and diffusivities of carbon dioxide in ionic liquids: [bmim][PF<sub>6</sub>] and [bmim][BF<sub>4</sub>]. *Ind. Eng. Chem. Res.* **2005**, *44*, 4453–4464.
- Hidden Isochema Ltd. www.isochema.com.
- Standard Test Method for Kinematic Viscosity of Transparent and Opaque Liquids and the Calculation of Dynamic Viscosity, ASTM method D445-88.
- Huddleston, J. G.; Visser, A. E.; Reichert, W. M.; Willauer, H. D.; Broker, G. A.; Rogers, R. D. Characterization and comparison of hydrophilic and hydrophobic room-temperature ionic liquids incorporating the imidazolium cation. *Green Chem.* **2001**, *3*, 156–164.
- Seddon, K. R.; Stark, A.; Torres, M.-J. Influence of chloride, water, and organic solvents on the physical properties of ionic liquids. *Pure Appl. Chem.* **2000**, *72* (12), 2275–2287.
- Van Valkenburg, M. E.; Vaughn, R. L.; Williams, M.; Wilkes, J. S. Ionic liquid heat transfer fluids. Presented at the 15th Symposium on Thermophysical Properties, June 22–27, 2003, Boulder, CO.
- Yokozeki, A. Time-dependent behavior of gas absorption in lubricant oil. *Int. J. Refrig.* **2002**, *22*, 695–704.
- Kato, R.; Krummen, M.; Gmehling, J. Measurement and correlation of vapor-liquid equilibria and excess enthalpies of binary systems containing ionic liquids and hydrocarbons. *Fluid Phase Equilib.* **2004**, *224*, 47–54.
- Döker, M.; Gmehling, J. Measurement and prediction of vapor-liquid equilibria of ternary systems containing ionic liquids. *Fluid Phase Equilib.* **2005**, *227*, 255–266.
- Anderko, A.; Wang, P.; Rafal, M. Electrolyte solutions: from thermodynamic and transport property models to simulation of industrial processes. *Fluid Phase Equilib.* **2002**, *194–197*, 123–142.
- Seiler, M.; Jork, C.; Kavarou, A.; Arlt, W.; Hirsch, R. Separation of azeotropic mixtures using hyperbranched polymers or ionic liquids. *AIChE J.* **2004**, *50*, 2439–2454.
- Van Ness, C. H.; Abbott, M. M. *Classical Thermodynamics of Nonelectrolyte Solutions*; McGraw-Hill: New York, 1982.
- Lemmon, E. W.; McLinden, M. O.; Huber, M. L. *A computer program, REFPROP (ver. 7)*; National Institute of Standards and Technology: Gaithersburg, MD, 2002.
- Walas, S. M. *Phase Equilibria in Chemical Engineering*; Butterworth: Stoneham, MA, 1985; pp 178–183.
- Reid, R. C.; Prausnitz, J. M.; Poling, B. E. *The Properties of Gases and Liquids*. 4th ed.; McGraw-Hill: New York, 1987.
- Hirschfelder, J. O.; Curtis, C. F.; Bird, R. B. *Molecular Theory of Gases and Liquids*; John Wiley: New York, 1964; p 1111.
- Yokozeki, A. Solubility and viscosity of refrigerant-oil mixtures. *Proc. Int. Compr. Eng. Conf. Purdue Univ.* **1994**, *1*, 335–340.
- Yokozeki, A.; Sato, H.; Watanabe, K. Ideal-gas heat capacities and virial coefficients of HFC refrigerants. *Int. J. Thermophys.* **1998**, *19* (1), 89–127.
- Asprion, N.; Hasse, H.; Maurer, G. FT-IR spectroscopic investigations of hydrogen bonding in alcohol-hydrocarbon solutions. *Fluid Phase Equilib.* **2001**, *186*, 1–25.
- Asprion, N.; Hasse, H.; Maurer, G. Application of IR-spectroscopy in thermodynamic investigations of associating solutions. *Fluid Phase Equilib.* **2003**, *205*, 195–214.
- Asprion, N.; Hasse, H.; Maurer, G. Thermodynamic and IR spectroscopic studies of solutions with simultaneous association and solvation. *Fluid Phase Equilib.* **2003**, *208*, 23–51.
- Crosthwaite, J. M.; Aki, S. N. V. K.; Maginn, E. J.; Brennecke, J. F. Liquid-phase behavior of imidazolium-based ionic liquids with alcohols: effect of hydrogen bonding and non-polar interactions. *Fluid Phase Equilib.* **2005**, *228–229*, 303–309.
- Geller, V.; Paulaitis, M.; Bivens, D. B.; Yokozeki, A. Transport properties and heat transfer of alternatives for R502 and R22. *Proc. ASHRAE/NIST Refrig. Conf.* **1996**, 73–78.

Received for review September 23, 2005. Accepted December 29, 2005. The present work was supported by DuPont Central Research and Development.

JE050386Z